**P1.6**

# A mechanism for convective initiation in advance of squall lines

Seung-hee Kim, Robert G. Fovell*, and Gretchen L. Mullendore
University of California, Los Angeles

## 1. Introduction

On 21 June 2003, a squall line traversed Oklahoma during the nighttime hours, continually spawning new convective cells ≈10-50 km ahead of the storm's gust front. The new cells were sufficiently close to the line to suspect a causal relationship between the new and existing convection, but also sufficiently removed to exclude gust front lifting as an initiation mechanism. Furthermore, the new convection aligned in lines that made an acute angle to the oncoming storm. Thus, we need to demonstrate an "action-at-a-distance" mechanism involving the existing convection, and to explain the orientation of the new cell lines relative to the existing storm.

Previous work (Fovell et al. 2004, 2006) has identified convectively-excited gravity waves as a potential link between old and new convection. These waves can be trapped beneath the existing storm's forward anvil as they propagate away, sparking the development of lower tropospheric shallow clouds ahead of the squall line. The organizing mechanism responsible for the orientation of the new cell lines is believed to be horizontal convective rolls (HCRs) that were present during the previous afternoon. The rolls decayed after sunset, but presumably left behind bands of moisture perturbations corresponding to the roll updraft and downdrafts.

We demonstrate the viability of this two-pronged mechanism with the help of idealized modeling. We create and control roll-like circulations and their associated moisture bands by introducing a momentum source in the boundary layer, and then permit a squall line to develop and evolve into a mature storm. In the future, environmental conditions such as the vertical shear will be manipulated to demonstrate the conditions under which gravity wave trapping is possible. The interaction between these waves and the moisture bands is examined for further insights into the important convective initiation question.

## 2. Observations

Figure 1 shows a series of base reflectivity scans from the Vance Air Force Base (VNX) radar taken during the early morning hours of 21 June 2003. A squall line having roughly north-south alignment can be seen moving towards the east. During this interval, a discrete line of new cells appeared, residing roughly 40 km ahead of the storm's main echo mass. This separation distance, though large, does not by itself preclude the gust front mechanism. However, surface temperature analyses from the Oklahoma Mesonet (superposed on the first two panels) and the appearance of a radar fine line (see arrows) place the gust front well to the west of the new cells.

Note that the new cell lines quickly take on a NW-SE orientation, thus making an acute angle to the bulk of the approaching storm. The new cells are translating eastward, but more slowly than the squall line, and development is slow, at least until they are underrun by the gust front (see circled cell at 0724Z). We believe the orientation of the new cell lines reflects the influence of HCRs that existed in this environment on the previous afternoon (Fig. 2). The rolls' vertical mixing creates bands of higher and lower humidity, aligned with the roll axes (e.g, Weckwerth et al. 1996; Dailey and Fovell 1999). The vertical motions in the rolls disappear after sunset as the boundary layer stabilizes, but one can reasonably suspect some of the moisture inhomogeneity survives, providing NW-SE oriented regions of more and less favorable air that persist into the nighttime hours.

## 3. Model setup

We hypothesize that the new cells seen on 21 June could have been provoked by gravity waves associated with the oncoming squall line that create new convective cells upon encountering residual moisture bands left behind by decayed HCRs. To demonstrate this idea, we made simulations with the Advanced Regional Prediction System (ARPS; Xue et al. 2000), version 4.5.2. The three-dimensional (3D) model domain extended 250 km in the nominal east-west ($x$) direction, spanned 100 km north-south ($y$), and was 18 km deep. Horizontal grid spacing was 1 km; the vertical grid spacing averaged 275 m, but was stretched to put the highest resolution in the lower troposphere. All boundaries except the model surface were open. The Weisman-Klemp (1982) thermodynamic profiles were used, with a surface layer vapor mixing ratio of 13.5 g kg$^{-1}$. We adopted warm rain microphysics for simplicity; the domain is fixed relative to the ground.

*Corresponding author address: Robert Fovell, UCLA Atmospheric and Oceanic Sciences, Los Angeles, CA 90095-1565. E-mail: rfovell@ucla.edu.

To simulate the effect of HCRs in a controlled fashion, we created "pseudo-rolls" by imposing a spatially-fixed streamfunction forcing in the boundary layer. Fovell (2005) used this technique to study gravity waves above roll-like obstacles. The streamfunction employed an 7 km roll spacing, a typical separation distance seen in HCR-associated roll clouds in the late afternoon (Kuettner 1971), and was confined to a finite region in the eastern half of the domain (see Fig. 3). On 21 June 2003, the roll clouds were oriented NW-SE, but for simplicity the forcing was aligned parallel to the $y$-axis. The streamfunction forcing was maintained for 5000 sec, and then deactivated.

Convection was initiated with a bubble placed in the domain's western half. To retain the angle observed between the storm and the new cell lines, the major axis of the bubble was oriented SW-NE (see Fig. 3). Random perturbations were superposed on this bubble to encourage 3D structures. The initial vertical wind profile (not shown) possessed no flow at the model surface, southerly shear below 1.5 km, and westerly shear between 1.5 and 3.5 km. HCRs tend to align parallel to the boundary layer shear vector, so this wind profile is compatible with the imposed forcing. A westerly jet was included between 7 and 10.5 km to enhance the forward anvil. The effect of excluding this jet has been examined.

## 4. Results and discussion

A squall line formed that organized largely along the bubble's major axis and propagated towards the east and south. Figure 4 shows the evolution of the near-surface potential temperature field, expressed as a perturbation from the base state, for a portion of the model domain. Superposed are selected cloud water contours from the 2.5 km level. Cloud water appeared at this level as the squall line approached. Small amounts of precipitation-sized particles formed in the new line between the times of panels b and c.

As in the observations, the new line drifted eastward after its appearance, but more slowly than the oncoming storm, permitting the latter to close the gap. The initially slab-like cloud line became more cellular with time (see Fig. 4d); whether this reflects its own development, or the influence of the oncoming storm, is not yet clear. Updrafts up to 15 m s$^{-1}$ (not shown) were present in the new cells at that time.

Figure 5 presents vertical cross-sections of cloud water and perturbation water vapor, at the location indicated on Fig. 4a. The squall line's gust front resided at about $x = 121$ km at the first time shown, far removed from the perturbations owing to the artificially-induced roll circulations ($x > 160$ km). In the upper troposphere, the forward anvil stretched ahead of the gust front by roughly 30 km. Beneath the anvil, eastward propagating vapor perturbations (or moisture bursts) are seen, associated with gravity waves excited by short-period variations in convective activity and trapped beneath the anvil (Fovell et al. 2006). One such moisture burst was propagating at about 35 m s$^{-1}$, far faster than the storm speed (14 m s$^{-1}$); it was excited at the gust front a few minutes prior to the time of Fig. 5a, when the new cell forming above the gust front started rapidly intensifying.

The relationship between the moisture bursts and gravity waves is illustrated in Fig. 6, taken from a simulation lacking roll forcing for the same time as Fig. 5b. Note that the wave vertical motions, and thus the moisture perturbations, decrease rapidly once the waves emerge from beneath the forward anvil, which serves to preserve and duct these features (Fovell et al. 2006). The ducting occurs due to both the decreased stability in the saturated anvil and the presence of a jet-like wind profile there. Thus, these transient bursts do not affect the roll perturbations significantly until the anvil starts passing overhead. That occurred around the time of Fig. 5c, when a burst encountered the roll perturbation identified by the arrow and helped it to become positively buoyant. This was the origin of the new cell line highlighted in Fig. 4.

Another view of this phenomenon is provided by Fig. 7, which shows the control run just before the cloud grew through the 2.5 km level shown in Fig. 4. The figure superposes the cloud outline at 2.25 km on the 6 km vertical velocity field. The trapped gravity waves excited by the squall line remained largely parallel to the established storm as they propagated away. The growth of the new cell line occurred as a gravity wave updraft passed over one of the pre-existing roll-induced moisture bands. Development commenced at the band's northern end because it was closer to the storm, and was thus influenced by the gravity wave first. As shown in Fig. 4, development subsequently proceeded all along the band; a similar phenomenon can be seen in the observations (Fig. 1; see also Fovell et al. 2004). The new line was subsequently advected eastward owing to the winds above the boundary layer. Fovell et al. (2004) showed that the new cells in the 21 June 2003 storm definitely resided beneath the approaching storm's anvil.

The simulations examined thusfar possessed an upper tropospheric westerly jet to enhance the storm's forward anvil. In this case, removal of that jet resulted in a storm with a far less extensive anvil outflow. In that simulation (not shown), no gravity waves that could propagate a significant distance ahead of the storm were produced, and no convective initiation occurred as the storm approached the rolls. Without an effective ducting mechanism, the gravity wave energy propagated away vertically. This result thus confirms that the prime location for convective initiation ahead of an established line is beneath its forward anvil, if present.

*Acknowledgments*. This work was supported by NSF grant ATM-0554765.

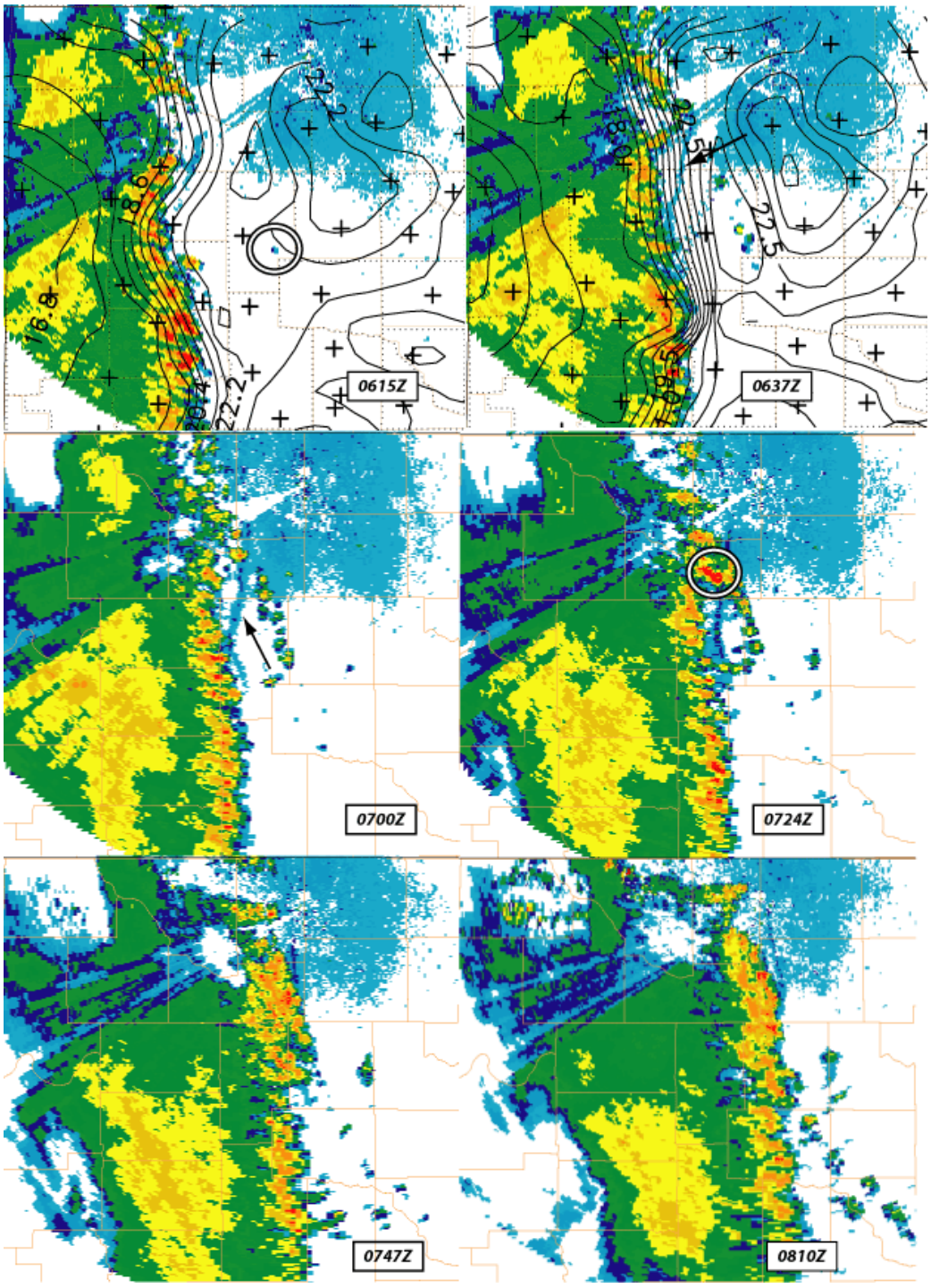


Fig. 1: Base reflectivity scans from the Vance Air Force Base (VNX) radar taken on 21 June 2003. On the first two panels, a surface temperature analyses (0.6°C contours) from the Oklahoma Mesonet data is superposed. Circle on the 0615Z panel marks first echo to appear along new discrete line present in right-hand panel; arrows point out probable gust front signatures. Plus signs mark mesonet station locations. After Fovell et al. 2004.

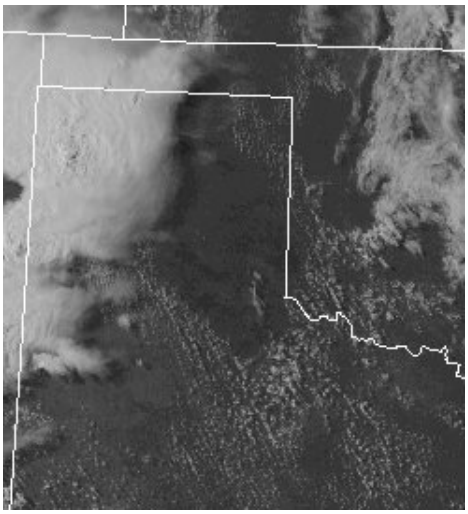

Fig. 2: Visible image from 2245Z (1745 local) on 20 June 2003, revealing NW-SE oriented cloud bands present over the Texas Panhandle and SW Oklahoma on the afternoon prior to the squall line passage. The developing line can be seen to the west.

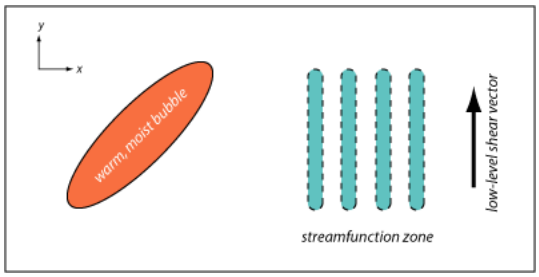


Fig. 3: Model setup schematic.

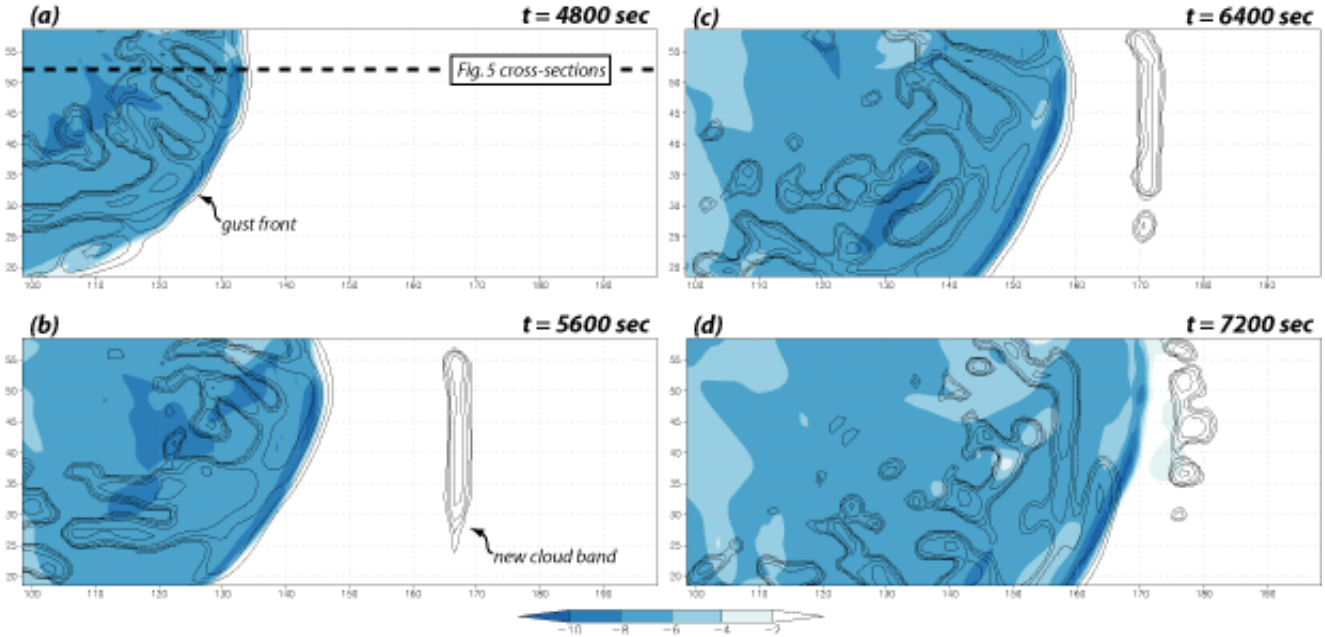


Fig. 4: Horizontal cross-section of near-surface perturbation potential temperature field (colored) from the control run, with selected cloud water contours from the 2.5 km level superposed. Cloud water contours are 0.125, 0.25, 0.5, 1.0, 2.0 and 4.0 g $kg^{-1}$. Only a 100 km by 20 km portion of the domain is shown.

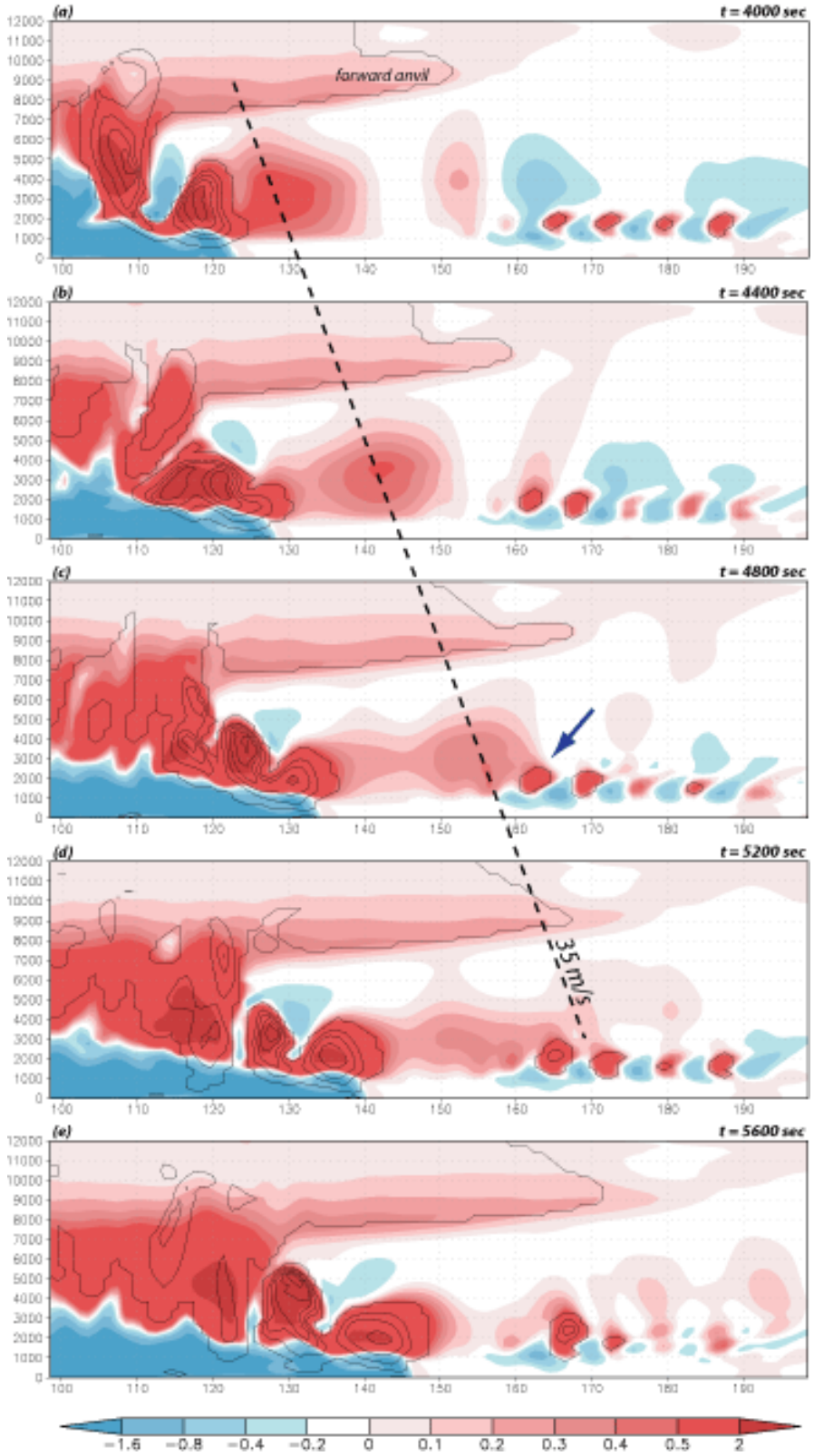


Fig. 5: Vertical cross-sections of perturbation vapor mixing ratio (colored) and cloud water (0.5 g $kg^{-1}$ contours) fields taken at the location indicated on Fig. 4a. Only a 100 km by 12 km portion of the domain is shown.

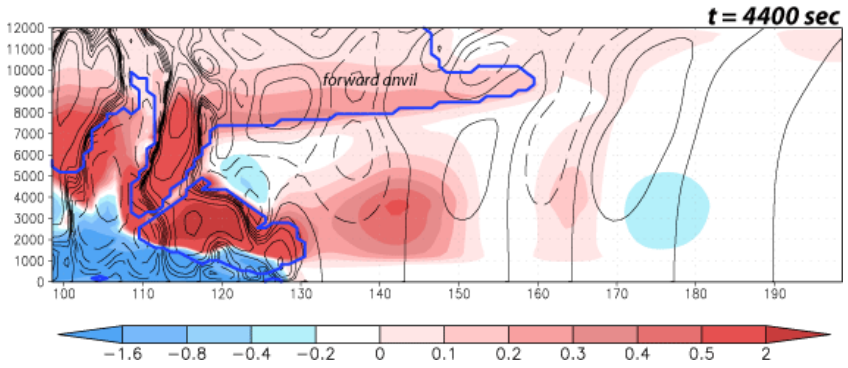


Fig. 6: Similar to Fig. 5b, but for a simulation lacking roll forcing. The contoured field is vertical velocity. Contours shown are ±0.5,1,2,4,8 and 16 m $s^{-1}$; negative contours dashed. Dark blue contour denotes the cloud outline.

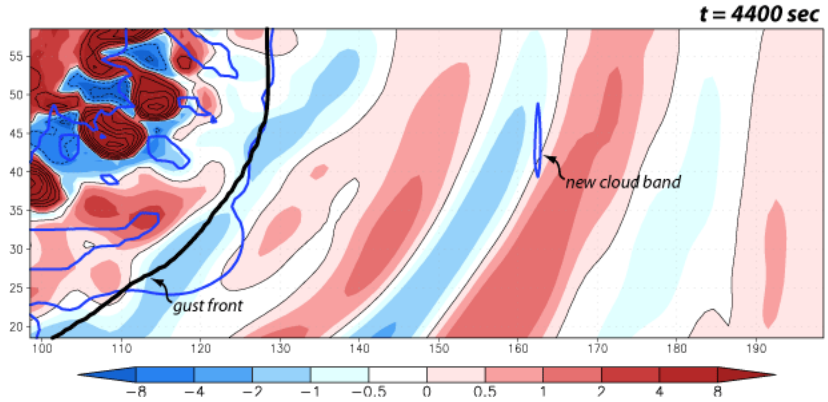


Fig. 7: Horizontal cross-section of vertical velocity at 6 km (colored), with gust front location superposed. Dark blue contour denotes the cloud outline at 2.25 km.

**References**


Dailey, P. S., and R. G. Fovell, 1999: Numerical simulation of the interaction between the sea-breeze front and horizontal convective rolls. Part I: Offshore ambient flow. *Mon. Wea. Rev.*, **127**, 858-878.

Fovell, R. G., 2002: Upstream influence of numerically simulated squall-line storms. *Quart. J. Roy. Meteor. Soc.*, **128**, 893-912.

——, 2005: Convective initiation ahead of the sea-breeze front. *Mon. Wea. Rev.*, **133**, 264-278.

——, and S.-H. Kim, 2003: Discrete Propagation in Numerically Simulated Nocturnal Squall Lines. Preprints, 10th Conf. on Mesoscale Processes, American Meteorological Society, unnumbered.

——, G. L. Mullendore and S.-H. Kim, 2006: Discrete propagation in numerically simulated nocturnal squall lines. *Mon. Wea. Rev.*, in press.

Kuettner, J. P., 1971: Cloud bands in the earth's atmosphere: Observations and theory. *Tellus*, **23**, 404-426.

Weckwerth, T. M., J. W. Wilson, and R. M. Wakimoto, 1996: Thermodynamic variability within the convective boundary layer due to horizontal convective rolls. *Mon. Wea. Rev.*, **124**, 769-784.

Weisman, M. L., and J. B. Klemp, 1982: The dependence of numerically simulated convective storms on vertical wind shear and buoyancy. *Mon. Wea. Rev.*, **110**, 504-520.

Xue, M., K. K. Droegemeier, and V. Wong, 2000: The Advanced Regional Prediction System (ARPS) - a multiscale, nonhydrostatic atmospheric simulation and prediction model. Part I: Model dynamics and verification. *Meteor. Atmos. Phys.*, **75**, 161-193.